Insights into Chagas treatment based on the potential of bacteriocin AS-48

Rubén Martín-Escolano[a], Rubén Cebrián[b,1], Javier Martín-Escolano[a], Maria J. Rosales[a], Mercedes Maqueda[b], Manuel Sánchez-Moreno[a], Clotilde Marín[a,*]

[a] Department of Parasitology, Instituto de Investigación Biosanitaria (ibs.Granada), Hospitales Universitarios De Granada/University of Granada, Severo Ochoa S/n, E-18071, Granada, Spain
[b] Department of Microbiology, Faculty of Sciences. C/ Fuentenueva S/n. University of Granada, Severo Ochoa /n, 18071, Granada, Spain

ARTICLE INFO

ABSTRACT

Chagas disease caused by the protozoan parasite *Trypanosoma cruzi* represents a significant public health problem in Latin America, affecting around 8 million cases worldwide. Nowadays is urgent the identification of new antichagasic agents as the only therapeutic options available, Nifurtimox and Benznidazole, are in use for > 40 years, and present high toxicity, limited efficacy and frequent treatment failures in the chronic phase of the disease. Recently, it has been described the antiparasitic effect of AS-48, a bacteriocin produced by *Enterococcus faecalis*, against *Trypanosoma brucei* and *Leishmania* spp. In this work, we have demonstrated the *in vitro* potential of the AS-48 bacteriocin against *T. cruzi*. Interesting, AS-48 was more effective against the three morphological forms of different *T. cruzi* strains, and displayed lower cytotoxicity than the reference drug Benznidazole. In addition, AS-48 combines the criteria established as a potential antichagasic agent, resulting in a promising therapeutic alternative. According to the action mechanism, AS-48 trypanocidal activity could be explained in a mitochondrion-dependent manner through a reactive oxygen species production and mitochondrial depolarization, causing a fast and severe bioenergetic collapse.

1. Introduction

Chagas disease (CD) caused by the flagellated protozoan *Trypanosoma cruzi* and transmitted by a triatomine insect is a neglected tropical disease endemic in Latin America. It is estimated that around 8 million people are infected worldwide and more than 28 million are living at risk of infection (WHO, 2016). The parasites can adopt three different morphological forms along their life cycle depending on the interaction with the host: i) epimastigote (the proliferative insect vector born stage), ii) trypomastigote (the infective, non-proliferative form) and iii) amastigote (intracellular proliferative form) (Adade et al., 2013). The main drugs used for the treatment of CD are Benznidazole (BZN, Rochagan®, Radanil®, Roche) and Nifurtimox (NFX, Lampit®, Bayer), which are ineffective in the chronic phase of the disease and present significant side effects (Adade et al., 2013). To this must be added the existence of strains resistant to these drugs, that hinders the disease treatment (Wilkinson et al., 2008; Mejia et al., 2012; Campos et al., 2014). For this reason, it is urgent to identify and develop novel active drugs against new targets, with low toxicity and high tolerance in patients, being effective in both, acute and chronic phase of the infection.

Resistance to antimicrobial compounds is a global phenomenon headed by bacteria. Because of this, antimicrobial peptides (AMPs) have been rediscovered for their potential use in the treatment of multidrug-resistant bacteria (Yu et al., 2016; Mishra et al., 2017; Lázár et al., 2018). AMPs can be defined as a ubiquitous and diverse group of natural compounds produced by all living organisms as a part of their innate defense system, that display antimicrobial activity against pathogen organism (Adermann et al., 2014; Smith and Dyrynda, 2015; Chung and Khanum, 2017; Kubicek-Sutherland et al., 2017). They are gaining attention in recent years due to their fast mode of action against a broad spectrum of pathogen microorganism and low capacity to generate resistance. The AMPs produced by bacteria are called bacteriocins. They are ribosomally synthesized peptides with antimicrobial activities (Hassan et al., 2012; Cotter et al., 2013). The mechanism of action is primarily based on the disruption of the cell membranes, although other mechanisms of action have been described (Prince et al., 2016). Due to the high specificity that they generally present towards the membranes of bacteria, in general, they present low toxicity and have been proposed as promising candidates for clinical and veterinary

---

use (Montalbán-López et al., 2011). Although their potential in the control of pathogenic bacteria is well documented, in the case of parasites not many studies are available. In fact, in the scientific literature there are some examples of AMPs with activity against *T. cruzi* either *in vitro* or *in vivo* (Amino et al., 2002; Jacobs et al., 2003; Fieck et al., 2010; Shin et al., 2016; Mello et al., 2017), however, to date, no bacteriocins with antiparasitic activity have been described.

One of the most exciting and well-known bacteriocin is the circular enterocin AS-48. It is a 70-residue, head-to-tail joined, amphipathic and cationic bacteriocin produced by different *Enterococcus* species (Maqueda et al., 2004) with a broad bactericidal activity against both Gram-positive and Gram-negative disease-associated pathogens (Gálvez et al., 1989; Aguilar-Pérez et al., 2018; Cebrián et al., 2018; Perales-Adán et al., 2018). The most distinctive structural feature of AS-48 is its circular structure and its amphipathicity, which contributes to a remarkable stability in a broad range of temperature and pH (Maqueda et al., 2004; Montalbán-López et al., 2011; Sánchez-Hidalgo et al., 2011). In addition, AS-48 exhibits very low immunogenicity and high resistance to exopeptidases (Maqueda et al., 1993).

The trypanocidal/leishmanicidal effect of AS-48 has been recently described. In both cases, the negative surface charge of the parasites has been related to the potent effect of AS-48. Although both parasites are from the same family, different action mechanisms have been described in each one (Abengózar et al., 2017; Martínez-García et al., 2018). The activity of AS-48 against *T. brucei* is the highest described until now, and it is because the high efficiency in the internalization of AS-48 by the flagellar pocket of the parasite. Although both parasites are from the same family, different action mechanisms have been described in each one (Abengózar et al., 2017; Martínez-García et al., 2018). In this study we report the *in vitro* activity of AS-48 against three different *T. cruzi* strains (including one BZN-resistant), investigating the putative mechanism of action. We have also demonstrated the low AS-48 cytotoxicity on uninfected Vero cells and the absence of pore-forming activity in both Vero cells and *T. cruzi*. Finally, AS-48 is a fast-acting cidal drug with an action mechanism that could be intermediate to those observed in *T. brucei* and *Leishmania* spp. In *T. cruzi* the trypanocidal activity could be mainly explained in a mitochondrion-dependent manner through the production of reactive oxygen species (ROS) and mitochondrial depolarization. In summary and according to with the positive results achieved in this work, AS-48 is shaping up as a promising therapeutic agent against Chagas disease, although it will be crucial to perform the *in vivo* studies, in order to know the effectiveness in both acute and chronic phases of the disease.

2. Material and methods

2.1. AS-48 purification

Bacteriocin AS-48 was purified to homogeneity from cultures of the *Enterococcus faecalis* UGRA10 strain (Ananou et al., 2008; Cebrián et al., 2012) by chromatographic passes (cationic interchange and reversed-phase high-performance liquid chromatography, RP-HPLC) as has been previously described (Cebrián et al., 2015). The protein concentration of the purified AS-48 was determined by measuring UV absorption at 280 nm a Nanodrop 2000 (Thermo Fisher Scientific. Waltham, MA, USA).

2.2. Drug susceptibility assays against Vero cells and T. cruzi forms

2.2.1. Vero cells culture and cytotoxicity tests

Vero cells (EACC number 84113001) were cultured in RPMI (Gibco®) with 10% (v/v) FBS heat-inactivated, at 37 °C in humidified 95% air and 5% CO_2 atmosphere. Cytotoxicity tests were assessed using the method previously described (Martín-Escolano et al., 2018) at dosages of 1000 to 1 μM of AS-48 and BZN. Briefly, cytotoxicity was tested using 96-well microtiter plates by seeding the cells at $1.25 \times 10^4 \, mL^{-1}$.

After 24 h of incubation, the cells were treated with AS-48 and BZN in 0.2 mL volumes in RPMI (Gibco®) with 1% (v/v) FBS heat-inactivated for 48 h. Subsequently, resazurin sodium salt (Sigma-Aldrich) was added, the plates were incubated for a further 24 h, and finally the trypanocidal activity was determined by absorbance measurements. The trypanocidal effect, using GraphPad Prism 6, was expressed as the inhibition concentration 50 (IC_{50}), i.e., the concentration required to result in 50% inhibition.

2.2.2. Epimastigote forms culture and in vitro activity assays

Three different *T. cruzi* strains were assessed: SN3 (IRHOD/CO/2008/SN3); Arequipa (MHOM/Pe/2011/Arequipa); and Tulahuen (TINF/CH/1956/Tulahuen), belonging to three discrete typing units (DTUs), I, V and VI, respectively. Epimastigote forms were cultured at 28 °C in RPMI (Gibco®) with 10% (v/v) FBS heat-inactivated, 0.03 M hemin and 0.5% (w/v) trypticase (BBL) (Kendall et al., 1990).

For the trypanocidal test, epimastigote forms were centrifuged in the exponential growth phase at 400 g for 10 min. Trypanocidal activity was determined according to the method previously described (Martín-Escolano et al., 2018) at dosages ranged from 50 to 0.02 μM of AS-48 and BZN. Briefly, tests were carried out by seeding the parasites at $5 \times 10^5 \, mL^{-1}$ after adding AS-48 and BZN in 0.2 mL volumes in 96-well microtiter plates at 28 °C for 48 h. Finally, resazurin sodium salt (Sigma-Aldrich) was added, and after 24 h of incubation, the same procedure as described in 2.2.1. Section was performed.

2.2.3. In vitro activity assays against intracellular amastigote forms

Trypanocidal activity against amastigote forms and the infectivity index were determined according to the method previously described (Martín-Escolano et al., 2018) at dosages of 50 to 0.02 μM of each drug. Briefly, tests were performed in 24-well microtiter plates with rounded coverslips by seeding the Vero cells at $1 \times 10^4 \, well^{-1}$ in RPMI (Gibco®) with 10% (v/v) FBS heat-inactivated, at 37 °C in humidified 95% air and 5% CO_2 atmosphere. After 24 h of incubation, the cells were infected with Vero cell-derived trypomastigotes at a multiplicity of infection (MOI) ratio of 1:10. After 24 h, non-phagocyted parasites were washed away, and after adding AS-48 and BZN in 0.5 mL volumes in RPMI (Gibco®) with 1% (v/v) FBS heat-inactivated. After 72 h of incubation, the trypanocidal activity was assessed by analyzing 500 host cells in methanol-fixed and Giemsa-stained preparations. The trypanocidal effect was determined using GraphPad Prism 6, as mentioned in 2.2.1. Section.

2.2.4. In vitro activity assays against extracellular bloodstream trypomastigote forms

Epimastigote forms maintained at 28 °C were induced to transform into metacyclic forms using Grace's Insect Medium (Gibco®), TAU and TAU3AGG mediums following the method previously described (Martín-Escolano et al., 2018). The obtained metacyclic trypomastigote forms were used to infect Vero cells, and the obtained Vero cell-derived trypomastigotes were used to infect BALB/c mice. Finally, bloodstream trypomastigotes (BTs) were obtained by cardiac puncture during the parasitaemia peak.

Trypanocidal activity was determined as described previously (Martín-Escolano et al., 2018) in 96-well microtiter plates by seeding the parasites at $2 \times 10^6 \, mL^{-1}$ in RPMI (Gibco®) with 10% (v/v) FBS heat-inactivated, and after addition of AS-48 and BZN at dosages of 100 to 0.2 μM in 0.2 mL volumes at 37 °C in humidified 95% air and 5% CO_2 atmosphere. After 24 h of incubation, resazurin sodium salt (Sigma-Aldrich) was added, and after another 4 h of incubation, the same process as described in 2.2.1. Section was performed.

2.3. Permeability tests of the plasma membrane of Vero cells by trypan blue

The permeability of Vero cells was determined using 24-well microtiter plates by seeding the cells at $2 \times 10^5 \, mL^{-1}$ after adding AS-48

at dosages of 5-, 10- and 25-fold higher than IC_{50} in 0.5 mL volumes at 37 °C in humidified 95% air and 5% CO2 atmosphere for 10, 30 and 60 min. Untreated Vero cells and Vero cells exposed to 0.1% (v/v) and 0.01% (v/v) Triton X-100 (TX-100) were also included as negative and positive controls, respectively. After incubations, Vero cells were collected, and the plasma membrane permeability was determined by adding trypan blue dye (Sigma-Aldrich) at 0.2% (final concentration) to the cell suspension and counting using an optical microscope and a hemacytometer counter.

2.4. Studies of the action mechanism

2.4.1. Determination of plasma membrane permeabilization by flow cytometry using propidium iodide (PI)

Alterations in membrane permeability of *T. cruzi* Arequipa epimastigote forms were detected by PI nucleic acid stain (Tiuman et al., 2014; Bustos et al., 2017). Membrane permeability was determined in 1.5 mL microtubes by inoculating the parasites at $1 \times 10^7 \, \text{mL}^{-1}$ after adding AS-48 at dosages of 10-, 20- and 50-fold higher than IC_{50} in 0.5 mL at 28 °C for 10, 30 and 60 min. After incubations, epimastigote forms were centrifuged, washed with PBS, and stained with 2 μg/mL PI dye (Sigma-Aldrich) in 0.5 mL at 28 °C for 10 min (Tiuman et al., 2014). Non-stained parasites, untreated parasites and parasites exposed to 0.01% (v/v) and 0.1% (v/v) TX-100 as negative and positive controls were also included. Finally, the parasites were collected, washed twice with cold PBS, and resuspended in 1 mL of cold PBS for fluorescence measurements by flow cytometry in a BECTON DICKINSON FACSAria III flow cytometer using a BECTON DICKINSON FACSDiva v8.01 software (2350 Qume Drive, San Jose, Palo-Alto, California) (λ_{EXC} = 488 nm, λ_{EM} = 620 nm).

2.4.2. Metabolite excretion test by proton nuclear magnetic resonance (^1H NMR)

Cultures of epimastigote forms ($5 \times 10^5 \, \text{mL}^{-1}$) in cell culture flasks were added of AS-48 at IC_{25} concentrations and then maintained at 28 °C for 72 h. Non-treated parasites (negative controls) were also included. The supernatants were then collected by centrifugation at 800*g* for 10 min to determine the excreted metabolites by ^1H NMR using a VARIAN DIRECT DRIVE 400 MHz Bruker spectrometer with an AutoX probe using D2O as previously described (Fernández-Becerra et al., 1997). The binning, normalizations and analyses were obtained using Mestrenova 9.0 software.

2.4.3. Mitochondrial dysfunction tests
2.4.3.1. Rhodamine 123 (Rho) and acridine orange (AO) assays by flow cytometry. The treated *T. cruzi* Arequipa epimastigote forms described in 2.4.2. Section were centrifuged, washed twice with PBS, and stained with 10 μg/mL Rho or AO dyes (Sigma-Aldrich) in 0.5 mL at 28 °C for 20 min (Sandes et al., 2014). Non-stained parasites and untreated parasites were also included as controls. After that, the parasites were collected, washed twice with cold PBS, and resuspended in 1 mL of cold PBS for fluorescence measurements by flow cytometry in a BECTON DICKINSON FACSAria III flow cytometer using a BECTON DICKINSON

FACSDiva v8.01 software (2350 Qume Drive, San Jose, Palo-Alto, California). The fluorescence intensities for Rho (mitochondrial membrane potential) and AO (nucleic acids) were measured as described elsewhere (Sandes et al., 2014).

2.4.3.2. MitoSOX™ Red assays by flow cytometry. Cultures of *T. cruzi* Arequipa epimastigote forms ($1 \times 10^7 \, \text{mL}^{-1}$) in 1.5 mL microtubes were stained with 0.5 μM MitoSOX™ Red dye (Invitrogen) in 0.5 mL at 28 °C for 30 min (Abengózar et al., 2017), and washed twice with PBS before the assay (Piacenza et al., 2007). AS-48 was added at 5 μM (Abengózar et al., 2017) at 28 °C for 10, 30 and 60 min. Non-stained parasites, untreated parasites and parasites exposed to 200 μM hydrogen peroxide were also included. Finally, epimastigote forms were processed as described in 2.4.1. Section to measure the fluorescence intensity for oxMitoSOX (ROS production) (λ_{EXC} = 510 nm, λ_{EM} = 580 nm) (Piacenza et al., 2007).

2.5. Statistical analyses

Data were recorded on a Microsoft Excel spreadsheet, and statistical analyses were performed by using IBM SPSS Statistics software (v. 21). The *t*-test for paired samples was used to verify whether there were differences between the assays used, with $p < 0.05$ considered statistically significant and with a 95% confidence level. Also statistical studies based on contingency tables (prevalence) were conducted, together with the × 2 test of the relationship between variables.

3. Results and discussion

3.1. AS-48 effects over T. cruzi growth in vitro

Currently, the genetic diversity of *T. cruzi* is extensively known being the parasite classified into seven DTUs that show different evolutionary relationships, epidemiological and ecological associations, tropism, pathogenesis, genotype, phenotype, and drug resistance (Zingales, 2018). Different concentrations of purified AS-48 bacteriocin (50–0.02 μM) were assayed against extracellular epimastigote, trypomastigote and intracellular amastigote forms of three strains of *T. cruzi* belonging to different DTUs – SN3, Tc I; Arequipa, Tc V; and Tulahuen, Tc VI – to evaluate its inhibitory activity using BZN as the reference. The IC_{50} values are presented in Table 1. Toxicity of AS-48 and BZN against uninfected Vero cells was also tested in parallel (Table 1), and the selectivity index (SI) (SI = IC_{50} Vero cells/IC_{50} extra- and intracellular forms) (Table 2) against *T. cruzi* was calculated.

In the case of the epimastigote forms, the $IC_{50}/72$ h values ranged between 0.76 μM for the Arequipa strain and 1.16 μM for the BZN resistant SN3 strain. These values were 22, 31 and 24-fold lower for Arequipa, SN3 and Tulahuen strains (respectively), than the values obtained for BZN.

Regarding the amastigote forms the relationship between the $IC_{50}/$ 72 h of BZN/AS-48 was lower (8, 2 and 5-fold) due to the minor susceptibility of these forms. The strains Arequipa and Tuhaluen were the most sensitive to AS-48 (0.99 and 1.98 μM respectively) while the strain

Table 1

Trypanocidal activity of AS-48 and BZN on the three developmental forms of *T. cruzi* strains. Toxicity on Vero cells.

Comp.	Activity IC_{50} (μM)[a]			Activity IC_{50} (μM)[a]			Activity IC_{50} (μM)[a]			Toxicity $IC_{50}/72$ h (μM)
	Arequipa strain			SN3 strain			Tulahuen strain			Vero cell
	E/72 h	A/72 h	T/24 h	E/72 h	A/72 h	T/24 h	E/72 h	A/72 h	T/24 h	
BZN	16.86 ± 1.81	8.25 ± 0.72	12.35 ± 1.14	36.51 ± 2.44	16.62 ± 1.46	36.09 ± 3.12	19.72 ± 1.75	9.96 ± 0.84	15.09 ± 1.30	80.35 ± 7.08
AS-48	0.76 ± 0.11	0.99 ± 0.13	0.17 ± 0.04	1.16 ± 0.18	6.81 ± 0.89	0.11 ± 0.02	0.82 ± 0.11	1.98 ± 0.22	0.19 ± 0.03	93.06 ± 5.67

[a] IC_{50} = concentration (μM) required to inhibit 50% population, calculated using GraphPad Prism 6. Results are averages of three separate determinations ± standard deviation. E, epimastigote forms. A, amastigote forms. T, trypomastigote forms.

Table 2
Selectivity Index for AS-48 and BZN on extra- and intracellular forms of *T. cruzi* strains.

Comp.	Selectivity index Arequipa strain[a]			Selectivity index SN3 strain[a]			Selectivity index Tulahuen strain[a]		
	E	A	T	E	A	T	E	A	T
BZN	4.77	9.73	6.51	2.20	4.83	2.23	4.07	8.07	5.32
AS-48	122.45	94.00	547.41	80.22	13.67	846.00	113.49	47.00	489.79
AS-48/BZN[b]	26	10	84	36	3	379	28	6	92

[a] Selectivity index (SI) = IC_{50} Vero cells/IC_{50} extracellular and intracellular form of parasite. [b]Number of times that AS-48 exceeds the reference drug SI (on extracellular and intracellular forms of *T. cruzi*). E, epimastigote forms. A, amastigote forms. T, trypomastigote forms.

SN3 showed a higher resistance (6.81 μM). We suggest that this could be due to AS-48 has to cross many membranes to reach the parasite, and the intracellular environment may not be the most appropriate for the AS-48 activity.

Finally, the trypomastigote forms were also susceptible to AS-48 treatment with the lower IC_{50}/24 h: 0.17, 0.11 and 0.19 μM against Arequipa, SN3 and Tulahuen strains, respectively, while BZN needed 12.35, 36.09 and 15.09 μM, respectively. Interesting, these forms were more the most resistant to BZN (not in the case of Arequipa) (Table 1) with an IC_{50}/24 h BZN/AS-48 ratio of 73, 328, and 79. The high AS-48 activity observed in these forms could be due to the characteristics of their membranes, which are composed mostly of phosphatidyl-choline and to a lesser extent of phosphatidyl-ethanol-amine (Agusti et al., 2000).

It is remarkable that BTs and intracellular amastigote forms are the most interesting forms from a clinical point of view (González et al., 2005) being in all cases sensitive to a low micromolar range of AS-48. In general, the IC_{50} observed for these forms were lower than the activity observed in the case of *Leishmania* spp. (IC_{50} of 4 μM and 10.2 μM for *L. donovani* and *L. pifanoi* promastigotes and amastigotes respectively). However, these IC_{50} were higher than in the case of *T. brucei* (1.7–3.12 nM) probably due to the fact that AS-48 is not able to enter inside *T. cruzi* as fast as in *T. brucei*. In fact, in the procyclic form of *T. brucei* or in the blood forms at 4 °C (when the parasite endocytic-membrane activity is stopped), the IC_{50} obtained for *T. brucei* were closed to the values obtained for *T. cruzi* (Martínez-García et al., 2018). These data make us think that the mechanism of action, in this case, could be intermediate between *Leishmania* spp. and *T. brucei*.

Furthermore, the toxicity towards Vero cells was also assayed. In this case, the IC_{50}/72 h was higher for AS-48 (93.06 μM) than for BZN (80.35 μM) (Table 1). The calculated AS-48 IC_{50} toward these cells confirmed, together with the IC_{50} values against the different forms of the parasite, a high selectivity index for the different morphological forms of *T. cruzi* tested, much better than the selectivity index observed for BZN (Table 2).

Moreover, to obtain accurate information about the AS-48 trypanocidal activity, *in vitro* infection on Vero cells and treatment with AS-48 was performed. The rate of infection of *T. cruzi* Arequipa strain was measured by counting infected cells after 72 h of exposure at different concentrations of AS-48. The data are shown in Fig. 1, together with the data of amastigote and trypomastigote forms. It was found that the rates of infected cells decreased as the concentrations of AS-48 increased, with an IC_{50}/72 h of 2.62 μM (6-fold lower than for BZN). Likewise, the total number of amastigote and trypomastigote forms decreased more for AS-48-treated cultures than for those treated with BZN.

The average number of amastigote forms per cell was also measured at different concentrations (Fig. 2), giving an idea of the killing rate. The data show that AS-48 is faster acting than BZN, which is considered until now as a fast-acting compound (Chatelain, 2015). These data show that AS-48 not only inhibits the parasite multiplication (static compound) but also causes its death (cidal compound). These features are additional advantages since fast-acting trypanocidal drugs can
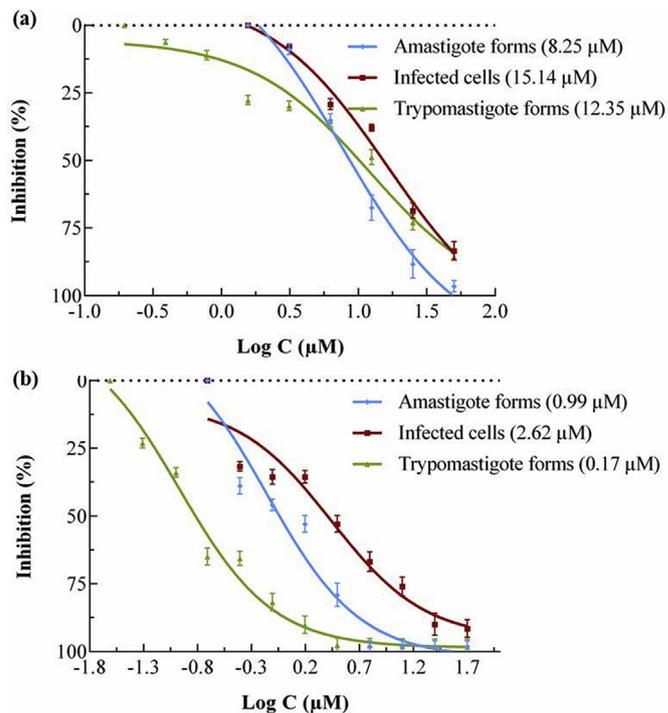
Fig. 1. Reduction of the infection of *T. cruzi* Arequipa strain regarding the decrease of amastigote and trypomastigote forms and infected cells treated with (a) BZN and (b) AS-48. Values are the means of three separate experiments ± standard deviation. In brackets: IC_{50} value, calculated using GraphPad Prism 6.
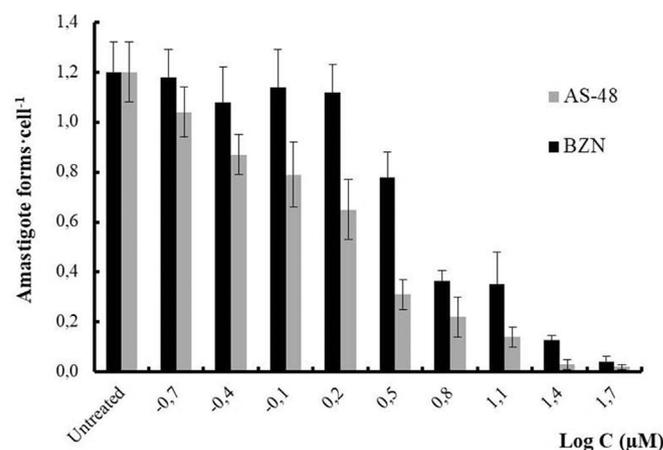
Fig. 2. Reduction in the number of amastigote forms of *T. cruzi* Arequipa strain per Vero cell treated with BZN and AS-48 for 72 h. Values are the means of three separate experiments ± standard deviation. Significant differences between the BZN and AS-48 for α = 0.05.
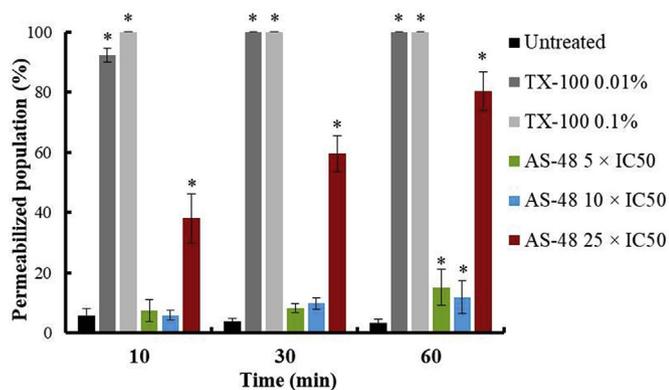
Fig. 3. Permeabilization of the plasma membrane of Vero cells treated with TX-100 and AS-48 for 10 min, 30 min and 60 min. Values are the means of the three separate determinations ± standard deviation. * Significant differences between untreated and treated Vero cells for α = 0.05.

Fig. 4. Permeabilization of the plasma membrane of epimastigote forms of *T. cruzi* Arequipa strain treated with TX-100 and AS-48 for 10 min, 30 min and 60 min. Values are the means of the three separate determinations ± standard deviation. * Significant differences between untreated and treated parasites for α = 0.05.

eliminate the parasite in a few doses (Rycker et al., 2012).

It is noticeable that in amastigote forms AS-48 has to go inside the cell to kill the parasite crossing the decks that surround it. This is the first time that has been reported activity for AS-48 inside of non-immune cells (different to macrophage in the case of *Leishmania* spp). In order to elucidate how AS-48 can enter into the Vero cells, a permeability membrane assay was performed at different AS-48 concentrations and exposure times, using TX-100 as control (Fig. 3 and SFig. 1). The tested AS-48 concentrations were higher than the IC_{50} obtained (Table 1) because the incubation times were shorter and a higher number of Vero cells were used for the test. The data show that AS-48 did not disrupt the Vero cells membranes at concentrations as high as 5- and 10-fold higher than IC_{50} – 191 and 382 μM, respectively – at 10 and 30 min and barely at 60 min, suggesting that AS-48 does not cause pores in spite of the high concentrations tested. Only those concentration very high tested (25-fold higher than IC_{50}, which is clote to 1 mM) seem to alter the Vero cells membranes, and never at the concentrations tested – 50 to 0.2 μM – in the activity assays against intracellular amastigote forms. With these results, the mechanism by which AS-48 can enter in the cell, without affect the integrity of the membrane barrier, and being able to kill the parasite, remains uncertain. However, one possibility is the cellular depolarization mechanism induced by cationic peptides when they are used at relevant concentrations, facilitating their entry through the membranes and activity on internal targets (Hale and Hancock, 2007).

Overall, these *in vitro* assays showed that AS-48 is a fast-acting and cidal agent that presents an excellent trypanocidal activity independent of the form and strain of the *T. cruzi* used, with higher activity and lower cytotoxicity than BZN. Moreover, AS-48 meets the *in vitro* criteria to be considered as a potential antichagasic agents: $IC_{50} \leq 10$ μM, and SI > 10 (Don and Ioset, 2014); or $IC_{50} < 5$ μM, SI > 10, and the majority of the *in vitro* criteria of the target product profile (TPP) (Chatelain, 2015).

3.2. Studies about the mechanism of action

3.2.1. AS-48 effects over T. cruzi plasma membrane pore-formation

According to the bactericidal and leishmanicidal mechanism of action described for AS-48, the primary target is the cell membrane where AS-48 forms pores (Sánchez-Barrena et al., 2003; Abengózar et al., 2017). To confirm if the fast-acting cidal effect observed for AS-48 on *T. cruzi* is also due to the formation of pores in the membrane, permeability assay of the plasma membrane of *T. cruzi* was performed by flow cytometry. We used PI stain after treating the parasites at different AS-48 concentrations and times of exposure, and TX-100 as positive control (Fig. 4 and SFig. 2). The AS-48 concentrations tested were higher than
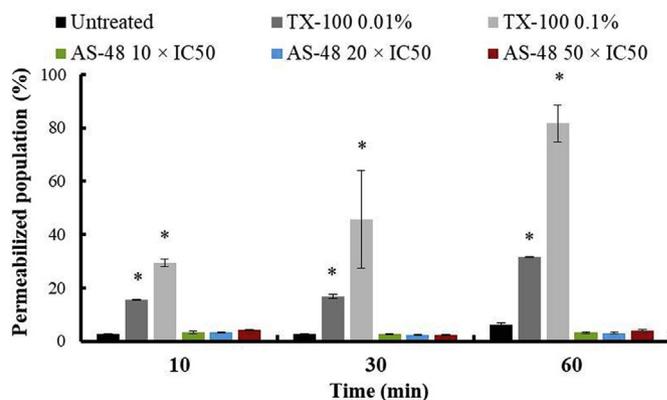
the IC_{50} obtained (Table 1) because the incubation times were shorter and more epimastigote forms were used. Collectively the data indicate that AS-48 did not permeate the *T. cruzi* plasma membrane at any of the concentrations (5-, 20- and 50-fold higher than IC_{50} – 3.8, 15.2 and 38 μM, respectively –) and incubation times tested, and therefore AS-48 must subject *T. cruzi* to a fast-acting cell death mechanism that differs from the pore formation. This suggests that as in *T. brucei*, AS-48 should enter in the parasite by endocytosis that in *T. cruzi* is restricted to two specialized invaginations of the plasma membrane, the flagellar pocket, and the cytostome (De Souza, 2008). Unlike *T. brucei* bloodstream forms, in which the endocytic turnover of the surface is exceptionally high, in *T. cruzi* the endocytic rate is much lower (Porto-Carreiro et al., 2000). The lower endocytic level has been also observed in amastigote forms, which could also be related to the higher resistance to AS-48 (Batista et al., 2015). Besides, cytostome is not present in trypomastigote forms (De Souza, 2008; Vidal et al., 2016), that according to our results are the most susceptible form. Therefore, the main route of entry of AS-48 into the cell should be the flagellar pocket.

The study of the mechanism of action at the energy metabolism level was evaluated. Alteration of metabolites excretion (glycosomal level) and also mitochondrial dysfunction (mitochondrial level) were prompted for three reasons: a) the strong AS-48 fast-acting trypanocidal effect (in the absence of a plasma membrane permeabilization) that can be caused by a fast and severe bioenergetic collapse, b) the single mitochondrion of *T. cruzi*, a likely target for AS-48 due to its evolutionary resemblance with bacteria, and c) the presence of cardiolipin, a typical mitochondrial phospholipid that interacts strongly with AS-48 (Gálvez et al., 1989).

3.2.2. Metabolite excretion

It is well-known that *T. cruzi* is unable to completely degrading glucose to CO_2 in aerobic environments, catabolizes glucose at a high rate, and acidifies the medium owing to incomplete oxidation to acids like pyruvate, acetate and succinate, among others (Bringaud et al., 2006). Consistently, to know the effect of AS-48 on glucose metabolism, ^1H NMR spectra of the medium of AS-48-treated epimastigote forms were qualitatively and quantitatively analyzed and compared with the spectra found for the untreated parasites (Fig. 5). The excretion of all metabolites in the three AS-48-treated *T. cruzi* strains was strikingly reduced concerning the corresponding untreated parasites. Therefore, a deficit in the production of catabolites by a blocking in the glycolytic pathway seems to be caused by AS-48. This alteration could be associated with an inhibition in the first enzymes involved in this pathway (glycosomal level) or to a mitochondrial dysfunction (mitochondrial level) that can produce an imbalance in the $NADH/NAD^+$ and ATP/
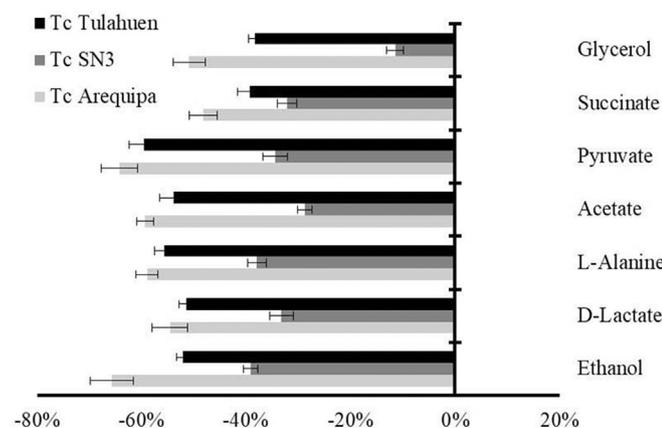
Fig. 5. Variation (percentages) among peaks of catabolites excreted by *T. cruzi* epimastigote forms exposed to AS-48 at their IC$_{25}$ in comparison to the control (untreated) incubated 72 h. Values are the means of three separate determinations $\pm$ standard deviation. Significant differences between the control and AS-48 for $\alpha = 0.05$.

ADP ratios causing a blockade in the glycolytic pathway (Bringaud et al., 2006; Wen et al., 2010).

3.2.3. Mitochondrial dysfunction

Hence, to assess if the alteration in the glycolytic pathway is a consequence of a mitochondrial dysfunction, flow cytometry analysis of the membrane potential and ROS production from treated parasites was performed using Rho and MitoSOX™ Red as fluorescents, respectively (Fig. 6, Fig. 7 and SFig. 3).

Regarding the mitochondrial membrane potential assay (Fig. 6), we confirmed that BZN-treated parasites showed a decrease in mitochondrial membrane potential (35.38%) because it is known that BZN kills *T. cruzi* through its transformation to highly reactive metabolites after reduction by type I nitroreductase activity (Hall and Wilkinson, 2012), causing, among others, respiratory chain inhibition. Interestingly, for AS-48, the treated parasites also showed a decrease in mitochondrial membrane potential (30.68%) despite having used a lower concentration (the IC$_{25}$).

Regarding the ROS production assay (Fig. 7 and SFig. 3), AS-48 treated parasites at 5 µM showed significant ROS production from 10 min of exposure (35.65%), being even higher than the parasites treated with H$_2$O$_2$, and increasing to more than 50% at 60 min of exposure.

3.2.4. Nucleic acids levels

The mitochondrion plays a crucial role in cell death decisions, and alterations in the integrity and function of it lead to a decrease in ATP production and nucleic acids levels, inducing apoptosis or necrosis (Lee and Thévenod, 2006; Shang et al., 2009). Therefore, the alterations observed in the integrity and function of the mitochondrion can lead to a decrease in ATP production and nucleic acids levels, inducing apoptosis or necrosis (Lee and Thévenod, 2006; Shang et al., 2009). Consequently, to determine the nucleic acids levels, flow cytometry analyses were performed using AO as fluorescent (Fig. 8). Remarkably, BZN and AS-48-treated parasites showed similar decreases in the AO fluorescence intensity (22.38% and 16.97%, respectively), as a consequence of the reduction in the amount of nucleic acids. It must be noted that the decrease in nucleic acids levels is also due to random nucleic acids degradation as commonly attributed feature to cell necrosis, and not only because of the APT deficit (Verma et al., 2007).

Accordingly, the putative mechanism of action for AS-48 could be explained in a mitochondrion-dependent manner through a mitochondrial depolarization and ROS production that causes a fast collapse in the energy metabolism of *T. cruzi*, as has been described in *Leishmania*
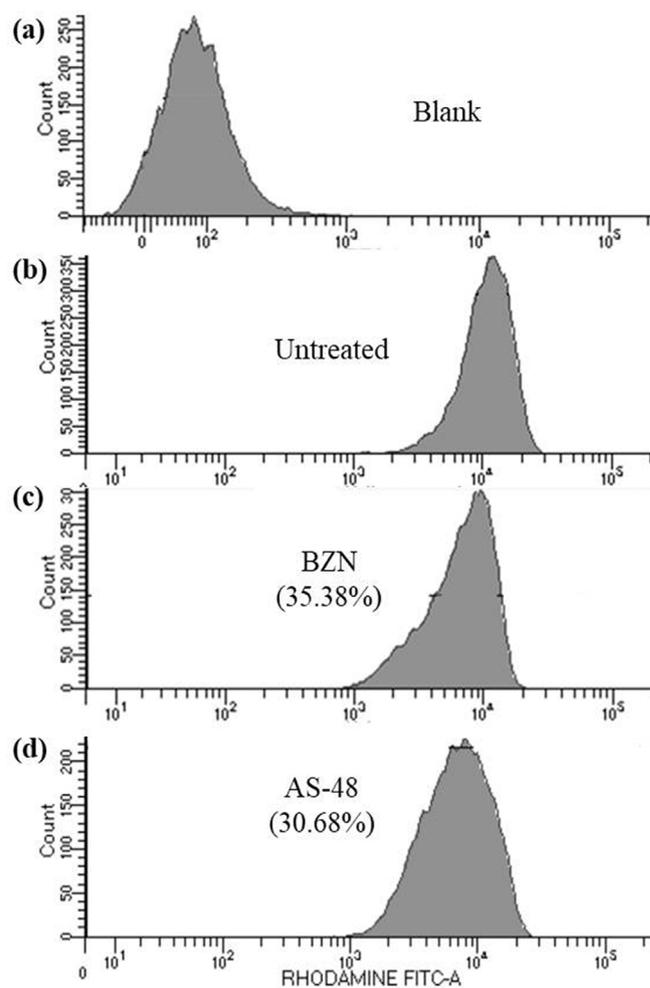
Fig. 6. Cytometry analysis of the mitochondrial membrane potential from epimastigotes of *T. cruzi* Arequipa strain exposed to BZN and AS-48 at their IC$_{25}$ in comparison to the control (untreated) incubated 72 h: (a) blank, (b) control (untreated), (c) BZN and (d) AS-48. Each drug was tested in three separate determinations. In brackets: reduction, in percentage, in the mitochondrial membrane potential with respect to untreated parasites. Significant differences between untreated parasites and parasites treated with BZN and AS-48 for $\alpha = 0.05$.
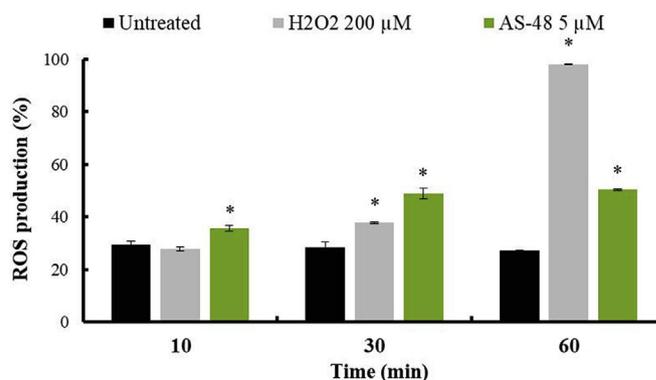
Fig. 7. Production of mitochondrial ROS of epimastigote forms of *T. cruzi* Arequipa strain exposed to H$_2$O$_2$ and AS-48 at 200 µM and 5 µM, respectively, for 10 min, 30 min and 60 min. Values are the means of the three separate determinations $\pm$ standard deviation. * Significant differences between untreated and treated parasites for $\alpha = 0.05$.
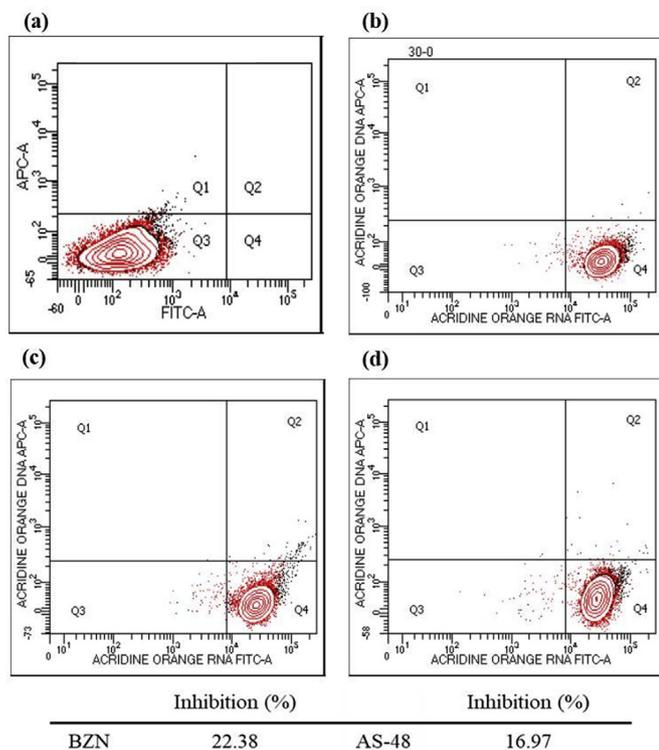
Fig. 8. Cytometry analysis showing the inhibition in the nucleic acids levels of epimastigotes of *T. cruzi* Arequipa strain exposed to BZN and AS-48 at their IC$_{25}$ in comparison to the control (untreated) incubated 72 h: (a) blank, (b) control (untreated), (c) BZN, (d) AS-48. Each drug was tested in three separate determinations. Below: reduction, in percentage, in the nucleic acids levels with respect to untreated parasites. Significant differences between untreated parasites and parasites treated with BZN and AS-48 for α = 0.05.

spp. (Abengózar et al., 2017). However, the AS-48 leishmanicidal activity is also produced by a partial plasma membrane permeabilization (Abengózar et al., 2017), a mechanism that does not happen in *T. cruzi*. We suggest that AS-48 should be endocytosed by the flagellar pocket. Moreover, the fact that intracellular amastigotes show a lower endocytosis activity than extracellular forms (Nogueira et al., 2015) also support their lower susceptibility of these to AS-48.

As AS-48 is a stable peptide that exhibits very low immunogenicity and high resistance to exopeptidases, it could be a promising drug against Chagas disease. Further validation of the usefulness of AS-48 in this field requires murine model assays to determine the *in vivo* trypanocidal activity of AS-48 during both the acute and chronic phases. Moreover, biochemical analysis will be performed in order to know the possible abnormalities associated with the treatments.

4. Conclusions

In conclusion, the trypanocidal properties of AS-48 were examined, and the experiments allowed us to present AS-48 as a promising alternative for the development of a new therapeutic agent against CD. AS-48 showed enhanced efficiency and lower toxicity than the reference drug BZN, and a broader spectrum of action. Finally, the action mechanism whereby AS-48 shows a fast-acting cidal effect against *T. cruzi* is mitochondrion-dependent through a ROS production and mitochondrial membrane depolarization, causing a fast and severe bioenergetic collapse. Interesting AS-48 has also displayed antiparasitic activity against amastigote forms (inside Vero cells) in a low micromolar range. This means that AS-48 has to enter in the cell to kill the parasite, being the first time that this kind of activity has been reported for a bacteriocin in non-defensive immune cells.

References

Adermann, K., Hoffmann, R., Otvos, L., 2014. IMAP 2012: antimicrobial peptides to combat (multi)drug-resistant pathogens. Protein Pept. Lett. 21, 319–320.
Abengózar, M.Á., Cebrián, R., Saugar, J.M., Gárate, T., Valdivia, E., Martínez-Bueno, M., Maqueda, M., Rivas, L., 2017. Enterocin AS-48 as evidence for the use of bacteriocins as new leishmanicidal agents. Antimicrob. Agents Chemother. 61, e02288-16.
Adade, C.M., Oliveira, I.R.S., Pais, J.A.R., Souto-Padrón, T., 2013. Melittin peptide kills *Trypanosoma cruzi* parasites by inducing different cell death pathways. Toxicon 69, 227–239.
Aguilar-Pérez, C., Gracia, B., Rodrigues, L., Vitoria, A., Cebrián, R., Deboosère, N., Song, O.R., Brodin, P., Maqueda, M., Aínsa, J.A., 2018. Synergy between circular bacteriocin AS-48 and ethambutol against. *Mycobacterium tuberculosis*. Antimicrob. Agents Chemother. 62, e00359-18.
Agusti, R., Couto, A.S., Alves, M.J.M., Colli, W., De Lederkremer, R.M., 2000. Lipids shed into the culture medium by trypomastigotes of *Trypanosoma cruzi*. Mem. Inst. Oswaldo Cruz 95, 97–102.
Amino, R., Martins, R.M., Procopio, J., Hirata, I.Y., Juliano, M.A., Schenkman, S., 2002. Trialysin, a novel pore-forming protein from saliva of hematophagous insects activated by limited proteolysis. J. Biol. Chem. 277, 6207–6213.
Ananou, S., Muñoz, A., Gálvez, A., Martínez-Bueno, M., Maqueda, M., Valdivia, E., 2008. Optimization of enterocin AS-48 production on a whey-based substrate. Int. Dairy J. 18, 923–927.
Batista, C.M., Kessler, R.L., Eger, I., Soares, M.J., 2015. *Trypanosoma cruzi* intracellular amastigotes isolated by nitrogen decompression are capable of endocytosis and cargo storage in reservosomes. PLoS One 10, e0130165.
Bringaud, F., Rivière, L., Coustou, V., 2006. Energy metabolism of trypanosomatids: adaptation to available carbon sources. Mol. Biochem. Parasitol. 149, 1–9.
Bustos, P.L., Volta, B.J., Perrone, A.E., Milduberger, N., Bua, J., 2017. A homolog of cyclophilin D is expressed in *Trypanosoma cruzi* and is involved in the oxidative stress-damage response. Cell Death Dis. 3, 16092.
Campos, M.C., Leon, L.L., Taylor, M.C., Kelly, J.M., 2014. Benznidazole-resistance in *Trypanosoma cruzi*: evidence that distinct mechanisms can act in concert. Mol. Biochem. Parasitol. 193, 17–19.
Cebrián, R., Baños, A., Valdivia, E., Pérez-Pulido, R., Martínez-Bueno, M., Maqueda, M., 2012. Characterization of functional, safety, and probiotic properties of *Enterococcus faecalis* UGRA10, a new AS-48-producer strain. Food Microbiol. 30, 59–67.
Cebrián, R., Martínez-Bueno, M., Valdivia, E., Albert, A., Maqueda, M., Sánchez-Barrena, M.J., 2015. The bacteriocin AS-48 requires dimer dissociation followed by hydrophobic interactions with the membrane for antibacterial activity. J. Struct. Biol. 190, 162–172.
Cebrián, R., Arévalo, S., Rubiño, S., Arias-Santiago, S., Rojo, M.D., Montalbán-López, M., Martínez-Bueno, M., Valdivia, E., Maqueda, M., 2018. Control of *Propionibacterium acnes* by natural antimicrobial substances: role of the bacteriocin AS-48 and lysozyme. Sci. Rep. 8, 11766.
Chatelain, E., 2015. Chagas Disease drug discovery: toward a new era. J. Biomol. Screen 20, 22–35.
Chung, P.Y., Khanum, R., 2017. Antimicrobial peptides as potential anti-biofilm agents against multidrug-resistant bacteria. J. Microbiol. Immunol. Infect. 50, 405–410.
Cotter, P.D., Ross, R.P., Hill, C., 2013. Bacteriocins - a viable alternative to antibiotics? Nat. Rev. Microbiol. 11, 95–105.
De Souza, W., 2008. An introduction to the structural organization of parasitic protozoa. Curr. Pharmaceut. Des. 14, 822–838.
Don, R., Ioset, J.R., 2014. Screening strategies to identify new chemical diversity for drug development to treat kinetoplastid infections. Parasitology 141, 140–146.
Fernández-Becerra, C., Sanchez-Moreno, M., Osuna, A., Opperdoes, F.R., 1997. Comparative aspects of energy metabolism in plant trypanosomatids. J. Eukaryot. Microbiol. 44, 523–529.
Fieck, A., Hurwitz, I., Kang, A.S., Durvasula, R., 2010. *Trypanosoma cruzi*: synergistic cytotoxicity of multiple amphipathic anti-microbial peptides to *T. cruzi* and potential bacterial hosts. Exp. Parasitol. 125, 342–347.
Gálvez, A., Maqueda, M., Martínez-Bueno, M., Valdivia, E., 1989. Bactericidal and bacteriolytic action of peptide antibiotic AS-48 against gram-positive and gram-negative

bacteria and other organisms. Res. Microbiol. 140, 57–68.

González, P., Marín, C., Rodríguez-González, I., Hitos, A.B., Rosales, M.J., Reina, M., Díaz, J.G., González-Coloma, A., Sánchez-Moreno, M., 2005. In vitro activity of C₂₀-di-terpenoid alkaloid derivatives in promastigotes and intracellular amastigotes of Leishmania infantum. Int. J. Antimicrob. Agents 25, 136–141.

Hale, J.D.F., Hancock, R.E.W., 2007. Alternative mechanism of action of cationic anti-microbial peptides on bacteria. Expert Rev. Anti Infect. Ther. 5, 951–959.

Hall, B.S., Wilkinson, S.R., 2012. Activation of benznidazole by trypanosomal type I ni-troreductases results in glyoxal formation. Antimicrob. Agents Chemother. 56, 115–123.

Hassan, M., Kjos, M., Nes, I.F., Diep, D.B., Lotfipour, F., 2012. Natural antimicrobial peptides from bacteria: characteristics and potential applications to fight against antibiotic resistance. J. Appl. Microbiol. 113, 723–736.

Jacobs, T., Bruhn, H., Gaworski, I., Fleischer, B., Leippe, M., 2003. NK-lysin and its shortened analog NK-2 exhibit potent activities against Trypanosoma cruzi. Antimicrob. Agents Chemother. 47, 607–613.

Kendall, G., Wilderspin, A.F., Ashall, F., Miles, M.A., Kelly, J.M., 1990. Trypanosoma cruzi glycosomal glyceraldehyde-3-phosphate dehydrogenase does not conform to the "hotspot" topogenic signal model. EMBO J. 9, 2751–2758.

Kubicek-Sutherland, J.Z., Lofton, H., Vestergaard, M., Hjort, K., Ingmer, H., Andersson, D.I., 2017. Antimicrobial peptide exposure selects for Staphylococcus aureus resistance to human defence peptides. J. Antimicrob. Chemother. 72, 115–127.

Lázár, V., Martins, A., Spohn, R., Daruka, L., Grézal, G., Fekete, G., Számel, M., Jangir, P.K., Kintses, B., Csörgő, B., Nyerges, Á., Györkei, Á., Kincses, A., Dér, A., Walter, F.R., Deli, M.A., Urbán, E., Hegedűs, Z., Olajos, G., Méhi, O., Bálint, B., Nagy, I., Martinek, T.A., Papp, B., Pál, C., 2018. Antibiotic-resistant bacteria show widespread collateral sensitivity to antimicrobial peptides. Nat. Microbiol. 3, 718–731.

Lee, W., Thévenod, F., 2006. A role for mitochondrial aquaporins in cellular life-and-death decisions? AJP Cell Physiol 291, C195–C202.

Maqueda, M., Gálvez, A., Martínez-Bueno, M., Guerra, I., Valdivia, E., 1993. Neutralizing antibodies against the peptide antibiotic AS-48: immunocytological studies. Antimicrob. Agents Chemother. 37, 148–151.

Maqueda, M., Gálvez, A., Bueno, M.M., Sanchez-Barrena, M.J., González, C., Albert, A., Rico, M., Valdivia, E., 2004. Peptide AS-48: prototype of a new class of cyclic bac-teriocins. Curr. Protein Pept. Sci. 5, 399–416.

Martín-Escolano, R., Moreno-viguri, E., Santivañez-Veliz, M., Martín-Montes, Á., Medina-Carmona, E., Paucar, R., Marín, C., Azqueta, A., Cirauqui, N., Pey, A.L., Pérez-Silanes, S., Sánchez-Moreno, M., 2018. Second generation of Mannich base-type derivatives with in vivo activity against Trypanosoma cruzi. J. Med. Chem. 61, 5643–5663.

Martínez-García, M., Bart, J.M., Campos-Salinas, J., Valdivia, E., Martínez-Bueno, M., González-Rey, E., Navarro, M., Maqueda, M., Cebrián, R., Pérez-Victoria, J.M., 2018. Autophagic-related cell death of Trypanosoma brucei induced by bacteriocin AS-48. Int. J. Parasitol. Drugs Drug Resist. 8, 203–212.

Mejia, A.M., Hall, B.S., Taylor, M.C., Gómez-Palacio, A., Wilkinson, S.R., Triana-Chávez, O., Kelly, J.M., 2012. Benznidazole-resistance in Trypanosoma cruzi is a readily ac-quired trait that can arise independently in a single population. J. Infect. Dis. 206, 220–228.

Mello, C.P., Lima, D.B., Menezes, R.R., Bandeira, I.C.J., Tessarolo, L.D., Sampaio, T.L., Falcão, C.B., Rádis-Baptista, G., Martins, A.M., 2017. Evaluation of the antichagasic activity of batroxicidin, a cathelicidin-related antimicrobial peptide found in Bothrops atrox venom gland. Toxicon 130, 56–62.

Mishra, B., Reiling, S., Zarena, D., Wang, G., 2017. Host defense antimicrobial peptides as antibiotics: design and application strategies. Curr. Opin. Chem. Biol. 38, 87–96.

Montalbán-López, M., Sanchez-Hidalgo, M., Valdivia, E., Martinez-Bueno, M., Maqueda, M., 2011. Are bacteriocins underexploited? NOVEL applications for OLD anti-microbials. Curr. Pharmaceut. Biotechnol. 12, 1205–1220.

Nogueira, P.M., Ribeiro, K., Silveira, A.C., Campos, J.H., Martins-Filho, O.A., Bela, S.R., Campos, M.A., Pessoa, N.L., Colli, W., Alves, M.J., Soares, R.P., Torrecilhas, A.C.,

2015. Vesicles from different Trypanosoma cruzi strains trigger differential innate and chronic immune responses. J. Extracell. Vesicles 4, 28734.

Perales-Adán, J., Rubiño, S., Martínez-Bueno, M., Valdivia, E., Montalbán-López, M., Cebrián, R., Maqueda, M., 2018. LAB bacteriocins controlling the food isolated (Drug-Resistant) staphylococci. Front. Microbiol. 9, 1143.

Piacenza, L., Irigoín, F., Alvarez, M.N., Peluffo, G., Taylor, M.C., Kelly, J.M., Wilkinson, S.R., Radi, R., 2007. Mitochondrial superoxide radicals mediate programmed cell death in Trypanosoma cruzi: cytoprotective action of mitochondrial iron superoxide dismutase overexpression. Biochem. J. 403, 323–334.

Porto-Carreiro, I., Attias, M., Miranda, K., De Souza, W., Cunha-e-Silva, N., 2000. Trypanosoma cruzi epimastigote endocytic pathway: cargo enters the cytostome and passes through an early endosomal network before storage in reservosomes. Eur. J. Cell Biol. 79, 858–869.

Prince, A., Sandhu, P., Ror, P., Dash, E., Sharma, S., Arakha, M., Jha, S., Akhter, Y., Saleem, M., 2016. Lipid-II independent antimicrobial mechanism of nisin depends on its crowding and degree of oligomerization. Sci. Rep. 6, 37908.

Rycker, M.D., O'Neill, S., Joshi, D., Campbell, L., Gray, D.W., Fairlamb, A.580H., 2012. A static-cidal assay for Trypanosoma brucei to aid hit prioritisation for progression into drug discovery programmes. PLoS Neglected Trop. Dis. 6 e1932.

Sánchez-Barrena, M.J., Martínez-Ripoll, M., Gálvez, A., Valdivia, E., Maqueda, M., Cruz, V., Albert, A., 2003. Structure of bacteriocin AS-48: from soluble state to membrane bound state. J. Mol. Biol. 334, 541–549.

Sánchez-Hidalgo, M., Montalbán-López, M., Cebrián, R., Valdivia, E., Martínez-Bueno, M., Maqueda, M., 2011. AS-48 bacteriocin: close to perfection. Cell. Mol. Life Sci. 68, 2845–2857.

Sandes, J.M., Fontes, A., Regis-da-Silva, C.G., Brelaz De Castro, M.C.A., Lima-Junior, C.G., Silva, F.P.L., Vasconcellos, M.L.A.A., Figueiredo, R.C.B.Q., 2014. Trypanosoma cruzi cell death induced by the Morita-Baylis-Hillman Adduct 3-Hydroxy-2-Methylene-3-(4-Nitrophenylpropanenitrile). PLoS One 9, e93936.

Shang, X.J., Yao, G., Ge, J.P., Sun, Y., Teng, W.H., Huang, Y.F., 2009. Procyanidin induces apoptosis and necrosis of prostate cancer cell line PC-3 in a mitochondrion-dependent manner. J. Androl. 30, 122–126.

Shin, J.M., Gwak, J.W., Kamarajan, P., Feno, J.C., Rickard, A.H., Kapila, Y.L., 2016. Biochemical applications of nisin. J. Appl. Microbiol. 120, 1449–1465.

Smith, V.J., Dyrynda, E.A., 2015. Antimicrobial proteins: from old proteins, new tricks. Mol. Immunol. 68, 383–398.

Tiuman, T.S., Ueda-Nakamura, T., Alonso, A., Nakamura, C.V., 2014. Cell death in amastigote forms of Leishmania amazonensis induced by parthenolide. 14, 152.

Verma, N.K., Singh, G., Dey, C.S., 2007. Miltefosine induces apoptosis in arsenite-resistant Leishmania donovani promastigotes through mitochondrial dysfunction. Exp. Parasitol. 116, 1–13.

Vidal, J.C., Alcantara, C.L., de Souza, W., Cunha-E-Silva, N.L., 2016. Loss of the cytos-tome-cytopharynx and endocytic ability are late events in Trypanosoma cruzi meta-cyclogenesis. J. Struct. Biol. 196, 319–328.

Wen, J.-J., Gupta, S., Guan, Z., Dhiman, M., Condon, D., Lui, C., Garg, N.J., 2010. Phenyl-α-tert-butyl-nitrone and Benzonidazole treatment controlled the mitochondrial oxi-dative stress and evolution of cardiomyopathy in chronic chagasic rats. J. Am. Coll. Cardiol. 55, 2499–2508.

Wilkinson, S.R., Taylor, M.C., Horn, D., Kelly, J.M., Cheeseman, I., 2008. A mechanism for cross-resistance to nifurtimox and benznidazole in trypanosomes. Proc. Natl. Acad. Sci. U.S.A. 105, 5022–5027.

World Health Organization (WHO), 2016. Chagas Disease (American Trypanosomiasis). (accessed 5.30.18). http://www.who.int/mediacentre/factsheets/fs340/en/.

Yu, G., Baeder, D.Y., Regoes, R.R., Rolff, J., 2016. Combination effects of antimicrobial peptides. Antimicrob. Agents Chemother. 60, 1717–1724.

Zingales, B., 2018. Trypanosoma cruzi genetic diversity: something new for something known about Chagas disease manifestations, serodiagnosis and drug sensitivity. Acta Trop. 184, 38–52.